Accepted Manuscript

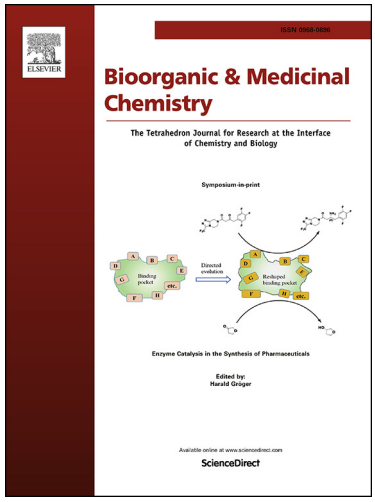

Synthesis and evaluation of aryliden- and hetarylidenfuranone derivatives of usnic acid as highly potent Tdp1 inhibitors

Olga Zakharova, Olga Luzina, Alexandra Zakharenko, Dmitry Sokolov, Alexandr Filimonov, Nadezhda Dyrkheeva, Arina Chepanova, Ekaterina Ilina, Anna Ilyina, Kristina Klabenkova, Boris Chelobanov, Dmitry Stetsenko, Ayesha Zafar, Chatchakorn Eurtivong, Jóhannes Reynisson, Konstantin Volcho, Nariman Salakhutdinov, Olga Lavrik

PII: S0968-0896(18)30657-6
DOI: https://doi.org/10.1016/j.bmc.2018.07.039
Reference: BMC 14476

To appear in: *Bioorganic & Medicinal Chemistry*

Received Date: 3 April 2018
Revised Date: 19 July 2018
Accepted Date: 22 July 2018

Please cite this article as: Zakharova, O., Luzina, O., Zakharenko, A., Sokolov, D., Filimonov, A., Dyrkheeva, N., Chepanova, A., Ilina, E., Ilyina, A., Klabenkova, K., Chelobanov, B., Stetsenko, D., Zafar, A., Eurtivong, C., Reynisson, J., Volcho, K., Salakhutdinov, N., Lavrik, O., Synthesis and evaluation of aryliden- and hetarylidenfuranone derivatives of usnic acid as highly potent Tdp1 inhibitors, *Bioorganic & Medicinal Chemistry* (2018), doi: https://doi.org/10.1016/j.bmc.2018.07.039

Synthesis and evaluation of aryliden- and hetarylidenfuranone derivatives of usnic acid as highly potent Tdp1 inhibitors

Olga Zakharova[a#], Olga Luzina[b#], Alexandra Zakharenko[a], Dmitry Sokolov[b], Alexandr Filimonov[b,c], Nadezhda Dyrkheeva[a], Arina Chepanova[a], Ekaterina Ilina[a], Anna Ilyina[c], Kristina Klabenkova[c], Boris Chelobanov[a,c], Dmitry Stetsenko[a], Ayesha Zafar[d], Chatchakorn Eurtivong[d], Jóhannes Reynisson[d], Konstantin Volcho[b,c], Nariman Salakhutdinov[b,c], Olga Lavrik[a,c,*]

[*]E-mail: lavrik@niboch.nsc.ru

[#]Equal contribution

[a] Novosibirsk Institute of Chemical Biology and Fundamental Medicine, Siberian Branch of the Russian Academy of Sciences, Novosibirsk, 630090, Russian Federation

[b] N. N. Vorozhtsov Novosibirsk Institute of Organic Chemistry, Siberian Branch of the Russian Academy of Sciences, Novosibirsk, 630090, Russian Federation

[c] Novosibirsk State University, Novosibirsk, 630090, Russian Federation

[d] School of Chemical Sciences, University of Auckland, New Zealand

ABSTRACT

Tyrosyl-DNA phosphodiesterase 1 (Tdp1) is a repair enzyme for stalled DNA-topoisomerase 1 (Top 1) cleavage complexes and other 3′-end DNA lesions. Tdp1 is a promising target for anticancer therapy, since it can repair DNA lesions caused by Top1 inhibitors leading to drug resistance. Hence, Tdp1 inhibition should result in synergistic effect with Top1 inhibitors. Twenty nine derivatives of (+)-usnic acid were tested for *in vitro* Tdp1 inhibitory activity using a fluorescent-based assay. Excellent activity was obtained, with derivative **6m** demonstrating the lowest IC_{50} value of 25 nM. The established efficacy was verified using a gel-based assay, which gave close results to that of the fluorescent assay. In addition, molecular modeling in the Tdp1 substrate binding pocket suggested plausible binding modes for the active analogues. The synergistic effect of the Tdp1 inhibitors with topotecan, a Top1 poison in clinical use, was tested in two human cancer cell lines, A-549 and HEK-293. Compounds **6k** and **6x** gave very promising results. In particular, **6x** has a low cytotoxicity and an IC_{50} value of 63 nM, making it a valuable lead compound for the development of potent Tdp1 inhibitors for clinical use.

1. Introduction

Developing inhibitors of DNA repair enzymes is a promising approach to improve anticancer therapy, particularly for drug-resistant tumors. Radiation and chemotherapy of cancer usually induce DNA lesions; however, tumors can be resistant, or develop resistance, during treatment. Tyrosyl-DNA phosphodiesterase (Tdp1) plays a crucial role in repair of DNA lesions formed by antitumor drugs such as the Top1 inhibitors camptothecin, topotecan and irinotecan, making Tdp1 a promising target for adjunctive cancer treatment.[1-3] A relatively small number of Tdp1 inhibitors[4-13] have been reported in literature; most of them exhibit moderate inhibiting activity, which makes discovering novel Tdp1 inhibitors a worthwhile undertaking. Natural products are an important source of compounds for the development of novel medicines, due to the high chemical diversity often lacking in libraries of synthetic molecules.[14,15] Indeed, a number of effective Tdp1 inhibitors were identified from natural products.[16-19] It has been previously demonstrated that selective inhibition of Tdp1 using terpene-coumarin based ligands (see analogue **1**, Fig. 1), has a synergistic effect with camptothecin on the viability of the MCF-7 breast cancer cell line.[18,20]

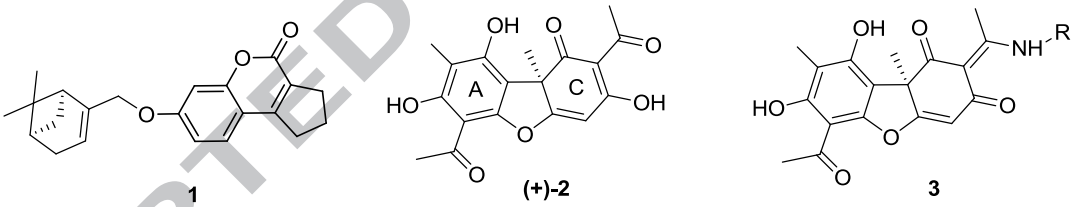

Fig. 1 Known Tdp1 coumarin based inhibitor **1**, usnic acid (+)-**2** and its derivative **3**.

Usnic acid is a secondary metabolite commonly found in various types of lichens, which has a broad range of biological activities: antiviral, antibiotic, analgesic, antimycotic and insecticide.[21,22] Research conducted over the past few decades has demonstrated that targeted synthesis of usnic acid derivatives yields various polycyclic compounds that exhibit potent biological activity for a number of important diseases, such as malaria, influenza and tuberculosis.[23-25]

It has been previously found that usnic acid derivatives, modified at ring C (general structure formula **3**, Fig. 1), are effective Tdp1 inhibitors with significant synergistic effect on the viability of the MCF-7 breast cancer cell line.[20] However, the presence of the native moieties on ring C is known to be important for the penetration of usnic acid derivatives through biological membranes.[26] This study aimed to synthesize and test the Tdp1 inhibitory activity of

usnic acid derivatives containing aryl- or hetarylidenfuranone moieties at ring A, keeping the triketone system in ring C of natural dibenzofurane intact.

2. Results and discussion

2.1. Chemistry

We have previously proposed the three-step synthesis scheme of benzylidenefuranone derivatives from (+)-usnic acid that included the stage of electrophilic bromination with bromine in dioxane giving bromoderivative **4**; subsequent intramolecular cyclization of compound **4** into furanone **5** in the presence of potassium hydroxide; and alkali-catalyzed condensation of **5** with appropriate aldehydes, resulting in compounds **6a-d**, **6h-k** (Scheme 1).[27]

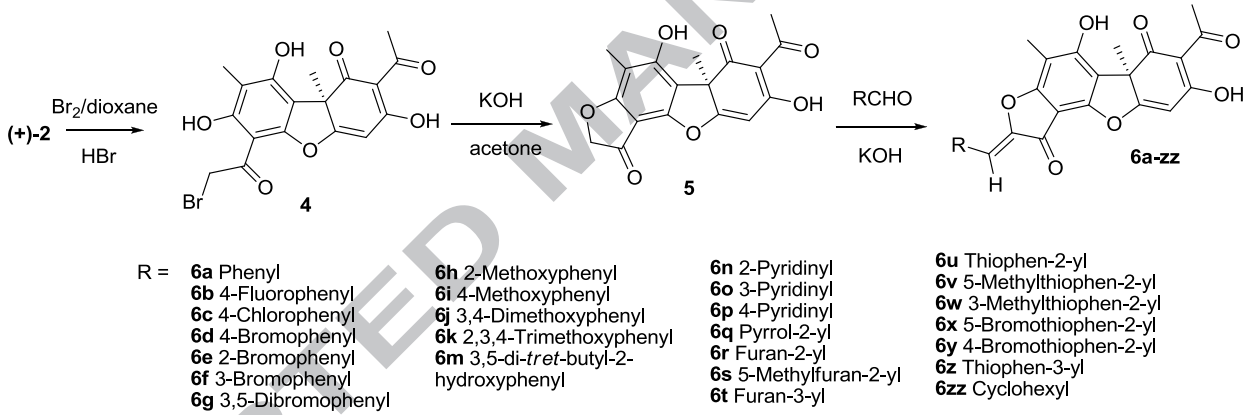

Scheme 1. The general reaction pathway for the furanones **6a-zz**.

Compounds **6a-k**, **m-z** (Table 1) as well as compound **6zz** with aliphatic substituent for structure activity relationship (SAR) purpose were successfully synthesized using this approach. Synthesis and NMR data of compounds **6a-d**, **6h-k**, **6n**, **6p** used in this study have been previously reported,[27,28] while, to the best of our knowledge, compounds **6e-g**, **6l**, **6m**, **6o**, **6q-zz** are new. Compounds **6e-g**, **6m**, **6o, 6q-zz** were synthesized by the reaction between compound **5** and appropriate aldehydes and isolated with the yields 30-94%. In order to synthesize compound **6l,** which contains a hydroxyl group at the *para*-position of the aromatic substituent, the hydroxyl group in 4-hydroxybenzaldhyde **7l** was first protected by reaction with 3,4-dihydro-2*H*-pyran (Scheme 2). After the reaction between compound **8l** and furanone **5**, the protective group in compound **9l** was removed by exposure to K-10 clay.

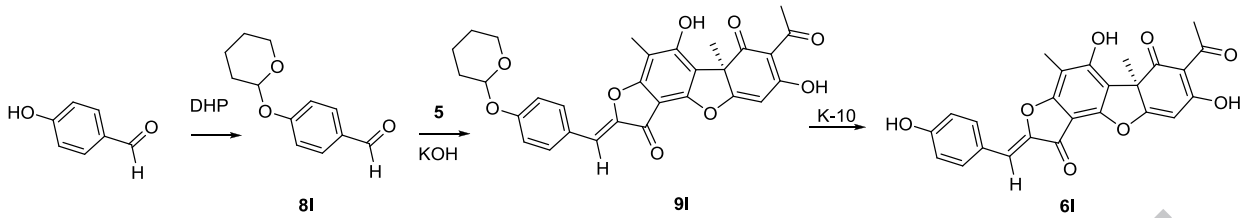

Scheme 2. The reaction pathway to compound **6l.**

In order to estimate the role of the alternate isomer of usnic acid in inhibitory activity, two isomeric compounds **7m** and **7x** were synthesized from (-)-usnic acid, following the same synthetic way as for the (+)-enantiomer (Scheme 3).

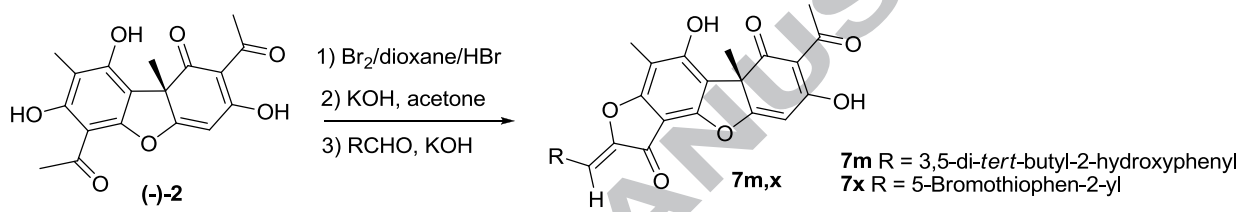

Scheme 3. The synthesis of compounds 7**m,x.**

The derivatives of usnic acid were evaluated for their Tdp1 inhibitory activity *in vitro*.

2.2 Biology

2.2.1 Inhibitory activity of compounds 6a-zz and 7m,x against Tdp1

We have recently designed an oligonucleotide biosensor for real-time detection of Tdp1 activity based on the ability of Tdp1 to remove fluorophore quenchers from the 3'-end of DNA.[10] The hexadecameric oligonucleotide carried 5(6)-carboxyfluorescein (FAM) at the 5'-end and the fluorophore quencher BHQ1 (Black Hole Quencher-1) at the 3'-end. Tdp1 inhibitors prevent removal of fluorophore quenchers, thus reducing fluorescence intensity.

The results from the Tdp1 assay for derivatives **6a-zz** and **7m**,**x** using the FAM-BHQ1 biosensor are shown in the Table 1.

For the phenyl-substituted compound **6a**, submicromolar activity (0.72 μM) was demonstrated. Among the halogen derivatives **6b-g**, compounds with one or more bromine atoms were the most active (IC_{50} = 0.15-0.53 μM), while fluoro- (**6b**) and chloro- (**6c**) derivatives appeared to be less active. The position of the bromine atom on the benzene ring did not significantly influence the activity of the inhibitors.

The introduction of the nitrogen atom into the aromatic ring does not affect the ability of the compounds to inhibit the enzyme (**6n-p,** IC_{50} values from 0.45 μM to 0.86 μM).

The addition of methoxy substituents in compounds **6h**, **6i** and **6k** increased activity approximately twofold (0.34-0.39 μM) in comparison with **6a**, though compound **6j**, with the 3,4-dimethoxyphenyl ring was less active. Replacement of the methoxy group by the hydroxyl group, when proceeding from **6h** to **6l**, decreased the activity fivefold.

Table 1. Inhibition of compounds **6a-zz, 7m** and **7x** on Tdp1 activity.

Compound	R	IC_{50}[a] μM	**Compound**	R	IC_{50}[a] μM
6a	Phenyl	0.72±0.08	**6n**	2-Pyridinyl	0.86±0.39
6b	4-Fluorophenyl	0.98±0.26	**6o**	3-Pyridinyl	0.45±0.07
6c	4-Chlorophenyl	1.22±0.15	**6p**	4-Pyridinyl	0.81±0.28
6d	4-Bromophenyl	0.15 ± 0.03	**6q**	Pyrrol-2-yl	3.65±1.38
6e	2-Bromophenyl	0.23±0.06	**6r**	Furan-2-yl	5.50±1.35
6f	3-Bromophenyl	0.232±0.004	**6s**	5-Methylfuran-2-yl	0.16±0.04
6g	3,5-Dibromophenyl	0.53±0.28	**6t**	Furan-3-yl	6.73±1.42
6h	2-Methoxyphenyl	0.39±0.13	**6u**	Thiophen-2-yl	0.90±0.17
6i	4-Methoxyphenyl	0.34±0.04	**6v**	5-Methylthiophen-2-yl	0.84±0.04
6j	3,4-Dimethoxyphenyl	1.02±0.18	**6w**	3-Methylthiophen-2-yl	0.63±0.29
6k	2,3,4-Trimethoxyphenyl	0.34±0.06	**6x**	5-Bromothiophen-2-yl	0.063±0.002
6l	4-Hydroxyphenyl	1.59±0.07	**6y**	4-Bromothiophen-2-yl	0.60±0.14
6m	3,5-Di-*tert*-butyl-2-hydroxyphenyl	0.025±0.002	**6z**	Thiophen-3-yl	3.30±1.05
6zz	Cyclohexyl	>15			
7m	3,5-Di-*tert*-butyl-2-hydroxyphenyl	0.064±0.021	**7x**	5-Bromothiophen-2-yl	0.081±0.011
Fur[b]		1.23±0.33			

[a] IC_{50} is the concentration that inhibits the activity of the enzyme by 50%.
[b] Fur is furamidine, diamidine NSC 305831, a commercial Tdp1 inhibitor,[6] which is used as a positive control.

At the same time, the most effective Tdp1 inhibitor from the compounds tested, with an excellent IC_{50} value of 25 nM, was **6m**, containing a large 3,5-di-*tert*-butyl-2-hydroxyphenyl substituent.

Compounds with a five-membered unsubstituted aromatic heterocycle (**6q, 6r, 6z**) were generally less potent Tdp1 inhibitors (IC_{50} values from 3.65 to 5.50 μM), excluding thiophen-2-yl derivative **6u**, with an IC_{50} of 0.9 μM. The insertion of the methyl group on the furan ring resulted in 35-fold increase in inhibitory activity (**6s** against **6q**). At the same time, the introduction of a methyl group or a bromine atom to the thiophene residue of thiophene-2-yl derivatives did not affect the inhibitory properties of the compounds (**6v, 6w, 6y**), with the exception of compound **6x**, which has a bromine atom at position 5. This modification led to a tenfold increase in the activity (IC_{50} 63 nM) in comparison with parent compound **6u** (IC_{50} 0.9 μM).

Compound **6zz,** containing a cyclohexyl substituent at the furanone ring instead of aryl or hetaryl substituents, was not active against Tdp1.

The influence of stereochemistry was studied using the most effective compounds, **6m** and **6x**, as examples. Their enantiomers, **7m** and **7x,** were synthesized from (-)-usnic acid and have the same effect on enzyme activity as found for the (+)-usnic acid derivatives (Table 1). Thus, the absolute configuration of the asymmetric center of the usnic acid does not influence inhibition potential.

Overall, most of the tested (het)arylidenfuranone derivatives of usnic acid demonstrated potent anti-Tdp1 activity in submicromolar, or even nanomolar, concentration.

2.2.2 Validation of Tdp1 inhibition by gel-based assay

In order to validate the results from the fluorescence-based assay by means of standard gel-based methods, we used two oligonucleotides of the same sequence 5'-d(AAC GTC AGG GTC TTC C) radiolabeled with [^{32}P] at the 5'-end, one containing fluorescence quencher BHQ1 and another containing a natural phosphotyrosine adduct at the 3'-end (Fig. 2). For the synthesis of the latter, a CPG (controlled pore glass) solid support was prepared, which incorporated *N*-Fmoc-tyrosine attached to an alkali-labile linker by its carboxyl group (Scheme 4). The oligonucleotide synthesis was started from the phenolic group of support-bound *N*-Fmoc-tyrosine.

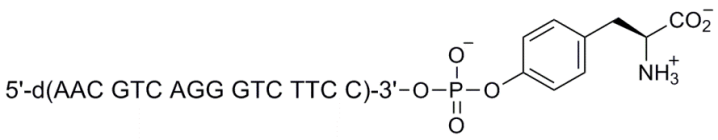

Fig. 2. The structure of the oligodeoxynucleotide with 3'-attached phosphotyrosine residue used as a Tdp1 substrate.

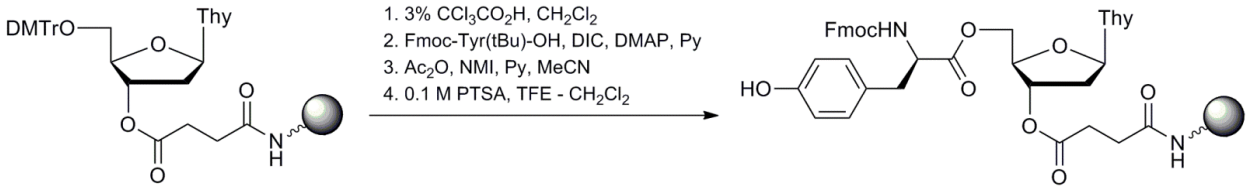

Scheme 4. The preparation of a CPG support with tyrosine attached to its carboxyl group by an ester bond.

Compound **6g**, which is active in submicromolar concentration, was chosen for this test. In the absence of an inhibitor, the enzyme cleaves the tyrosine residue (Fig.3A, lane 1), and the amount of product decreases with increasing concentration of inhibitor (Fig.3A, lanes 2-6). In the case of BHQ1, similar products were observed (data not shown). Fig.3B shows the amount of product as function of inhibitor concentration. The IC_{50} values were determined for compound **6g**, by the gel electrophoresis method, to be 0.64±0.33 μM for the 3'-BHQ1 substrate and 4.0±1.1 μM for the 3'-tyrosine substrate. For the 3'-BHQ1 substrate, the IC_{50} value was virtually identical to the one obtained using the fluorescence based assay (0.53±0.28 μM).

Both fluorescent and gel-based assays yield close results for 3'-BHQ1 substrate but differ by an order of magnitude for the 3'-tyrosine substrate. Taking into account that different substrates were used in the experiments, it can be concluded that very close results were obtained.

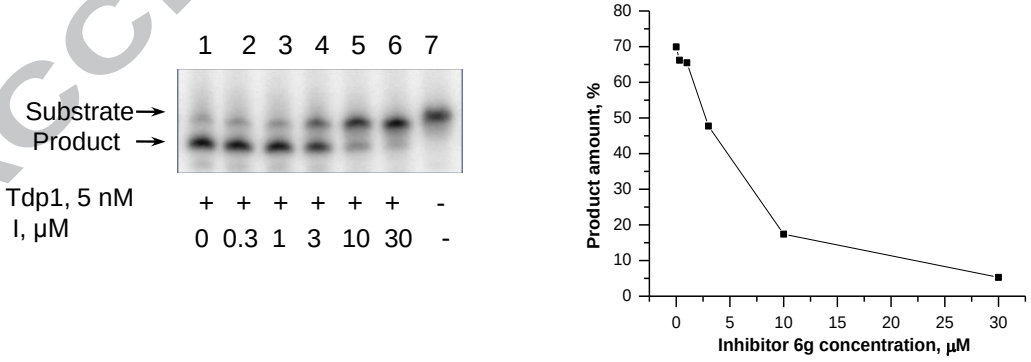

A **B**

Fig. 3 (A) Gel-electrophoresis autoradiogram of Tdp1 products on 3'-tyrosine substrate. 50 nM 5'-radiolabeled DNA substrate was reacted with 5 nM Tdp1 and indicated concentration of inhibitor **6g** at 25°C. "I" designates inhibitor (B). Plot of the amount of product as a function of the inhibitor concentration.

2.2.3 Cytotoxicity

It is desirable that the inhibitors have low toxicity, which would simplify their use as a component of "cocktails" with known anticancer drugs. The cytotoxicity of selected Tdp1 inhibitors was assessed using the A-549 adenocarcinomic human alveolar basal epithelial cells and HEK-293 embryonic kidney cells. The cells were incubated in the presence of the inhibitors at concentrations ranging from 1 to 100 μM. The diagrams of the survival rate of cells vs inhibitor concentration are shown in Figure 4.

To study cytotoxicity on A-549 and HEK-293 cells, the most effective Tdp1 inhibitors were selected (**6d, 6e, 6f, 6i, 6k, 6m, 6s,** and **6x)**. The compounds proved to be moderately toxic for the cells (CC_{50} values in the range from 4.6 to 20 μM, see Table 2) except for compound **6s**, for which CC_{50} value could not be determined for both cell lines (>50 μM).

Topotecan (**tpc**) is a bioavailable derivative of camptothecin, a topoisomerase 1 (Top1) inhibitor. **Tpc** is an important chemotherapeutic drug in the treatment of different cancer types.[29-31] To check for synergy of Top1 and Tdp1 inhibition, the cytotoxic effect of **tpc** in the presence of the Tdp1 inhibitors were tested. The nontoxic concentration of 1 μM was used in conjunction with varied concentrations of **tpc** to derive CC_{50} values.

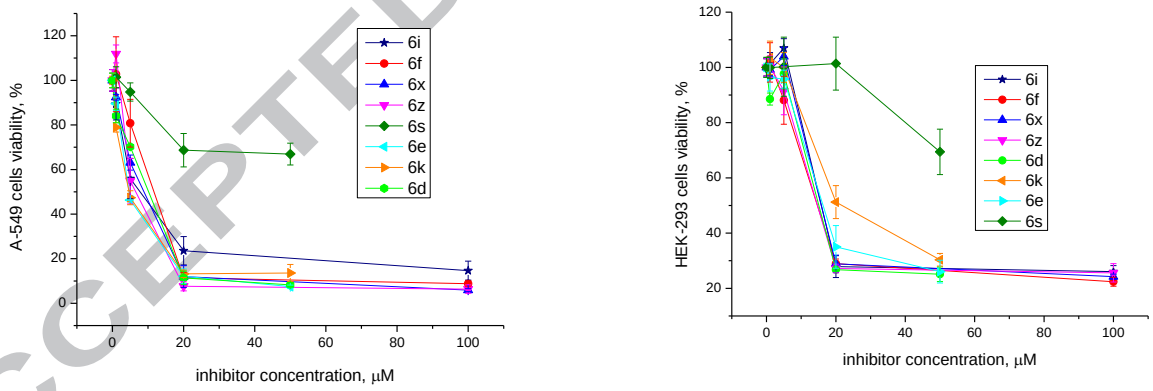

A **B**

Fig. 4. The influence of selected Tdp1 inhibitors on A-549 (A) and HEK-293 (B) cell viability.

MTT tests showed a twofold reduction of CC_{50} values for **tpc** in A-549 cells with **6e, 6k, 6s,** and **6x**, and a two- to fourfold reduction of CC_{50} values for **tpc** in HEK-293 cells with **6d, 6f, 6k** and **6x**, as shown in Figure 5 and Table 2. Compounds **6d, 6f** and **6i** had minor influence on **tpc** cytotoxicity for A-549 cells and compounds **6e, 6i, 6m** and **6s** had marginal effect on **tpc** cytotoxicity for HEK-293 cells. Surprisingly, the most effective Tdp1 inhibitor, **6m**, increased the value of CC_{50} of **tpc** five-fold for A-549 cells, thereby protecting the cells from the action of the drug. In addition, **6m** barely affected the cytotoxicity of **tpc** on HEK-293 cells. Two

compounds enhanced **tpc** cytotoxicity on both cell lines: **6k** and **6x**. Compound **6k** has quite a low selectivity index (the CC_{50} / IC_{50} ratio) (~60), whereas the SI of **6x** is 250 for the HEK-293 cell line. To summarize, we do not observe a correlation between the efficiency against the purified enzyme, the intrinsic cytotoxicity of the compounds, and their ability to enhance the effect of topotecan. Probably, it is related to the presence of other targets in the cells, such as PARP1 or Tdp2. As compound **6x** both enhances the effect of **tpc** and has a high SI, it is a promising candidate for further development.

Table 2. The IC_{50} values of the usnic acid derivatives, their A-549 and HEK-293 cell viabilities and selectivity indices (SI), as well as the cell viability in conjunction with **tpc**, a Top1 poison.

Compound	R	IC_{50}[a] μM	CC_{50} A-549[b] μM	SI[c]	CC_{50} HEK-293[b] μM	SI[c]	**tpc** CC_{50} A-549 nM[d]	**tpc** CC_{50} HEK-293 nM[d]
tpc							111±27	24±1
6d	4-Bromophenyl	0.15	10.0±0.4	66.7	14.6±0.5	97.3	162±66	10±3
6e	2-Bromophenyl	0.23	4.56±0.08	19.8	15.9±1.5	69.1	48±18	21±6
6f	3-Bromophenyl	0.232	11.4±2.3	49.1	14.5±0.7	62.5	132±10	10±2
6i	4-Methoxyphenyl	0.34	8.3±3.6	24.4	15.8±0.6	46.5	90±34	22±6
6k	2.3.4-Trimethoxyphenyl	0.34	4.6±0.4	13.5	20±2	58.8	48±3	5.3±0.5
6m	3.5-Di-*tert*-butyl-2-hydroxyphenyl	0.025	6.8±2.4	272	14.5±0.7	180	558±39	16±6
6s	5-Methylfuran-2-yl	0.16	>50	>300	>50	>300	40±4	22±6
6x	5-Bromothiophen-2-yl	0.063	8.7±1.0	138	15.7±0.5	249	47±5	13±6

[a] IC_{50} - 50% inhibition concentration.
[b] CC_{50} - median cytotoxic concentration causing 50% cell death.
[c] SI selectivity index, the CC_{50} / IC_{50} ratio.
[d] In the presence of 1 μM of Tdp1 inhibitor

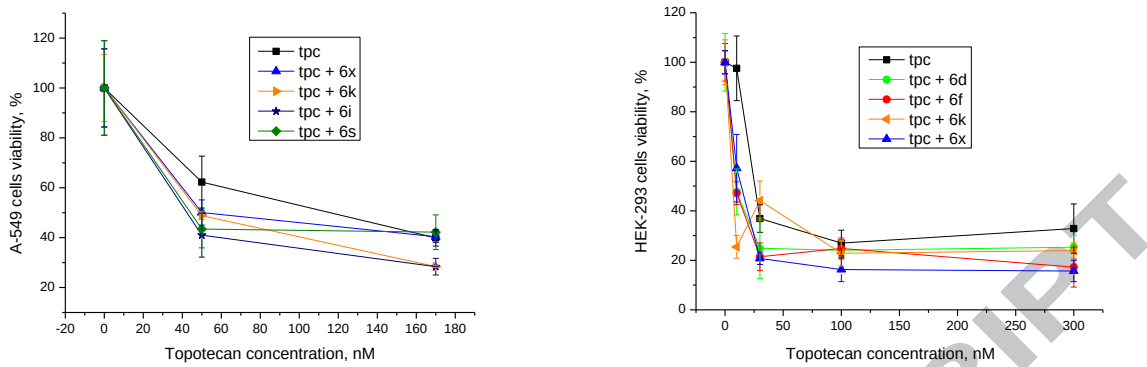

A **B**

Fig. 5. Dose-dependent action of **tpc** in combination with the **furanone derivatives of usnic acid** on A-549 (A) and HEK-293 (B) cell viability.

2.3 Molecular modeling

Recently, Tdp1 was proposed to have two distinct binding sites: the substrate and an allosteric binding pocket. This was based on molecular dynamic simulations for usnic acid derivatives, including compound of general formula **3** (Fig. 1).[20] Until now, the substrate pocket has been considered to be the binding site of Tdp1 inhibitors.[32] The molecular modeling work was aimed to establish the preferential binding sites and modes of binding for the usnic acid derivatives using docking (see experimental section for further detail). The derivatives were docked to both the substrate pocket and the allosteric binding cavity. The scores and IC_{50} values are shown in Table 3.

The computed affinity scores were based on four different algorithms: GoldScore (GS),[33] ChemScore (CS),[34,35] Piecewise Linear Potential (ChemPLP)[36] and Astex Statistical Potential (ASP).[37] There were no obvious correlations between the IC_{50} values and the scores. The four algorithms predicted higher scores for the inhibitors docked to the substrate binding pocket compared to the allosteric cavity on all occasions except one (derivative **6m** for ChemPLP). This suggests higher affinity and more preferential binding of the usnic acid derivatives to the substrate binding pocket. Furthermore, pose predictions of the four scoring functions was consistent for the substrate pocket, while more variation was seen for the allosteric cavity.

Table 3. The scores predicted by docking the usnic acid derivatives to the allosteric and substrate binding sites of Tdp1. Their IC_{50} values are also given.

Com-pound	IC_{50} (μM)	GS		CS		ChemPLP		ASP	
		Allosteric	Substrate	Allosteric	Substrate	Allosteric	Substrate	Allosteric	Substrate
6a	0.72	37.7	52.5	20.4	29.1	44.6	61.6	25.8	37.3
6b	0.98	37.5	52.1	19.9	29.1	47.0	58.1	26.6	37.3
6c	1.22	39.2	53.3	21.4	30.6	49.0	58.0	27.7	38.3
6d	0.15	43.7	52.8	20.8	29.8	48.6	59.5	25.5	37.3
6e	0.23	40.2	53.4	21.0	30.6	48.6	63.6	25.6	36.2
6f	0.232	42.3	55.4	21.4	30.5	49.1	58.2	24.1	37.2
6g	0.53	47.2	56.5	22.3	31.8	49.4	54.2	24.8	33.5
6h	0.39	45.0	52.0	21.3	31.0	49.9	59.5	27.3	35.9
6i	0.34	42.9	54.1	19.6	29.5	48.9	57.7	25.9	38.5
6j	1.02	46.3	53.6	19.7	29.4	51.5	61.5	26.4	38.7
6k	0.34	43.2	57.9	19.8	28.4	50.2	56.7	29.1	34.5
6l	1.59	41.4	51.7	18.4	27.1	52.4	57.4	28.1	36.6
6m	0.025	48.8	63.1	22.2	28.3	59.6	52.2	28.9	38.6
6n	0.86	45.1	50.1	20.1	30.8	51.5	61.3	26.8	39.2
6o	0.45	40.8	51.2	21.8	33.1	52.9	63.4	26.6	39.3
6p	0.81	43.5	49.8	20.4	30.6	52.2	62.4	28.5	38.2
6q	3.65	45.1	49.1	21.8	30.5	48.1	60.1	25.7	38.2
6r	5.5	43.0	48.0	21.7	30.6	51.5	58.4	25.8	37.9
6s	0.16	46.3	49.1	20.6	31.2	49.8	61.1	27.2	36.7
6t	6.73	37.9	48.2	19.5	32.4	51.4	63.1	25.4	39.9
6u	0.90	40.6	50.2	20.7	30.6	49.9	60.7	24.9	37.2
6v	0.84	44.1	53.1	21.1	31.7	51.3	61.9	25.2	37.2
6w	0.63	43.1	55.1	20.4	30.4	49.6	62.2	25.1	36.2
6x	0.063	46.6	51.9	21.9	31.1	51.3	61.8	26.3	36.4
6y	0.60	45.1	52.1	21.8	31.2	50.6	61.4	26.6	36.1
6z	3.30	45.8	51.1	21.3	30.8	52.6	62.8	24.6	37.1
6zz	> 15	44.1	50.0	21.3	30.3	43.4	59.4	24.1	35.1
7m	0.064	45.6	53.1	20.4	28.6	49.7	55.1	26.5	36.3
7x	0.081	49.9	55.4	22.6	31.4	53.1	62.5	26.2	39.9

Tdp1 catalyzes the hydrolysis of the Top1 tyrosine residue that is covalently linked by its phenolic group to the 3'-phosphate of DNA.[9,38] The catalytic mechanism involves the formation and hydrolysis of a Tdp1-DNA intermediate.[34] These catalytic steps are mediated by the protonation and deprotonation of the His263 and His493 residues and are crucial for the function of Tdp1.[9,38] Hence, a promising inhibition strategy is to disrupt the catalytic functions of His263 and His493. As an example, derivative **6m** (Fig. **6**) forms hydrogen bonds with His263 and Asn516 residues. The heterocyclic ring system is buried in the hydrophobic groove of the substrate binding pocket, depicted by the grey regions, and can form favorable hydrophobic contacts with the Tyr204, Pro461 and His493 amino acid residue side chains.

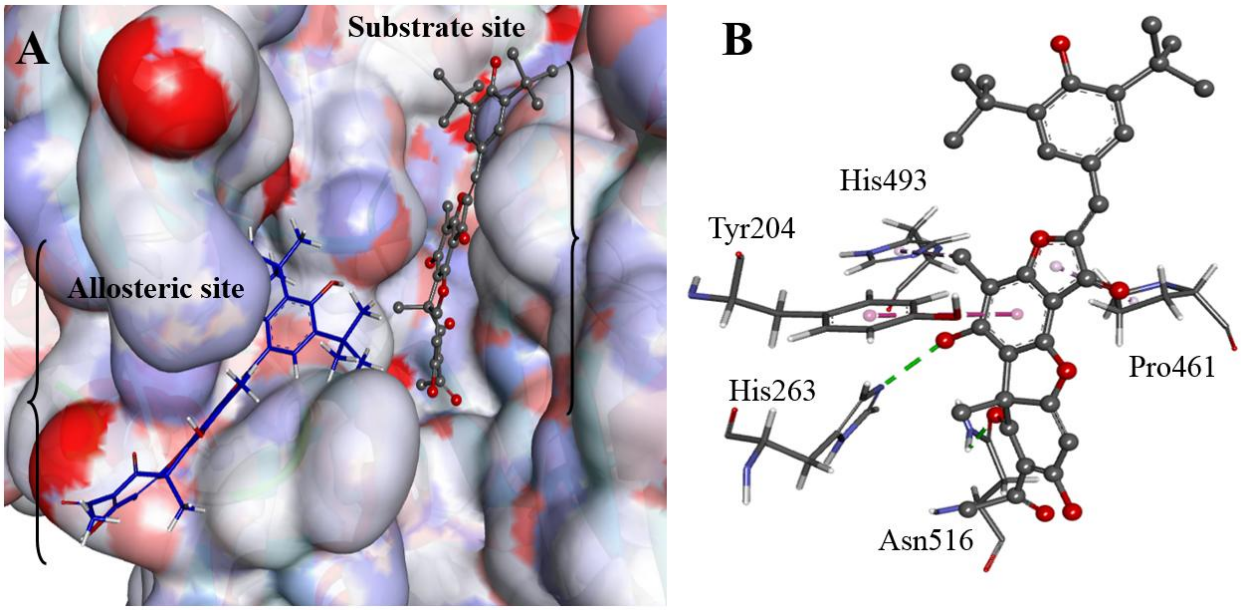

Figure 6. **(A)** Docked configurations of derivative **6m** to the allosteric and substrate binding sites predicted by the ChemPLP algorithm. The protein surface is rendered with partial positive charges colored as blue, negative charges are red and neutral regions are grey. The hydrogen atoms are removed for clarity. **(B)** The hydrogen bond interactions are depicted as green dotted lines between compound **6m** and amino acids residues His263 and Asn516 in the substrate binding pocket. Furthermore, lipophilic contacts (LC) are shown as purple dashed lines with His493, Tyr204 and Pro461.

The 3,5-di-tert-butylphenol moiety is an extension from the heterocycle located near Ile285. The kink shape of the usnic acids caused by the double bond allows the aryl moiety to fit into the concave shape of the groove (Fig. **6A**). In general, an excellent binding mode is predicted for the investigated ligand.

According to the modeling, the methyl groups of **7m** and **7x** are easily accommodated by the substrate binding pocket, which explains their similar IC_{50} values to the **6m**, **x** enantiomers.

2.3.1. Chemical space

The calculated molecular descriptors (MW – molecular weight, Log P – water / 1-octanol partition coefficient, HD – hydrogen bond donors, HA – hydrogen bond acceptors, PSA – polar surface area and RB – rotatable bonds) for the twenty nine derivatives are given in SI (**Table**). The ligands are relatively large, with molecular weight between 419.4 and 588.2. **6d, 6e**, **6f**, **6g**, **6k**, **6m**, **6x** and **6y** derivatives lie in the *Known Drug Space* region while others are within the boundaries of *drug-like space* (for definitions of *lead-like*, *drug-like* and *Known Drug Space* regions see ref).[39] Also, **6j**, **6k** and **6l** lie within the *Known Drug Space*. The log P values range from 1.9 to 4.7 and the rest of the descriptors adhere to the definition of *drug-like* chemical space.

3. Conclusion

Twenty nine usnic acid derivatives **6a-zz, 7m** and **7x** were synthesized, and evaluated for their *in vitro* Tdp1 inhibitory activity using a fluorescent based assay, which was verified with a gel-based assay for analogue **6g**. It was found that the absolute configuration of the asymmetric center in usnic acid derivatives does not influence inhibitory activity of the compounds.

Compounds **6a-z, 7m** and **7x** exhibited very high to moderate inhibitory activity (IC_{50} = 0.025 – 6.7 μM), compared to the presently known inhibitors. An excellent selectivity index was obtained for **6x,** which had a moderate cytotoxicity profile and potent inhibition of Tdp1. Furthermore, **6x** proved to be a **tpc** sensitizer for the A-549 and HEK-293 cell lines, with twofold enhancement of cytotoxicity of topotecan in non-toxic concentration. It should be mentioned that the lack of correlation between the efficiency of inhibition of the purified enzyme, cytotoxicity and the ability to sensitize to the effect of topotecan may indicate the presence of additional targets in a cell other than Tdp1.

Docking investigation predicted higher affinity and more preferential binding to the substrate binding pocket for the usnic acid derivatives compared to a potential adjacent allosteric cavity. This study identified a number of potential lead molecules that can aid in the development of drug candidates that enhance the potency of the Top 1 poisons in clinical use.

4. Experimental section

4.1. Chemistry

The analytical and spectral studies were conducted in the Chemical Service Center for the collective use of SB RAS.

The ^{1}H and ^{13}C NMR spectra for solutions of the compounds in $CDCl_3$ were recorded on a Bruker AV-400 spectrometer (400.13 and 100.61 MHz, respectively). The residual signals of the solvent were used as references (δ_H 2.48, δ_C 39.52). The mass spectra (70 eV) were recorded on a DFS Thermo Scientific high-resolution mass spectrometer. The melting points were measured using a Kofler heating stage. The specific rotation was determined on a PolAAr 3005 and provided in $(deg \times mL) \times (g \times dm)^{-1}$, where the concentration of the solutions is shown in $g \times (100 \times mL)^{-1}$. Merck silica gel (63-200 μ) was used for the column chromatography. Thin-layer chromatography was performed on Silufol plates (UV-254).

The atom numerations in the compound are provided for the assignment of signals in the NMR spectra and are different from the atom numerations in the nomenclature name. The target compounds reported in this manuscript have a purity of at least 97% (HPLC).

(*R*)-(+)-Usnic acid (+)-**2** (α_D +478 (c 0.1, $CHCl_3$)) was isolated by the procedure of Salakhutdinov et al.[40] from a mixture of lichens of the *genus Usnea*. (*S*)-(-)-Usnic acid (-)-**2** ($[\alpha]_D$ -458 (*c* 0.1, $CHCl_3$) was isolated by the same procedure from *Cladonia stellaris*.

Compounds **6a-d, 6h-k** were synthesized by the procedure described in [27].

Compounds **6n and 6p** were synthesized by the procedure described in [24].

4.1.1 Synthesis of compounds 6e-g, 6m, 6o, 6q-zz. General procedure.

Usnic acid **2** (1 mmol, 344 mg) was treated with the bromine–dioxane complex (2 mmol Br_2, 0.10 mL, dissolved in dioxane, 14 mL) and several drops of HBr then left for 7 d at room temperature. The reaction mixture was concentrated in a rotary evaporator and chromatographed over silica gel with elution by CH_2Cl_2 to yield compound **4** (67%).

A solution of **4** (1 mmol, 423 mg) in acetone (25 mL) was treated with KOAc (150 mg, 1.5 mmol), refluxed for 2 h, diluted with H_2O (up to ~50–60 mL), acidified with HCl (1:4) to pH 3–4, and extracted with CH_2Cl_2 (3 - 10 mL). The extracts were dried over calcined $MgSO_4$. The solvent was removed. The residue was chromatographed over a column of silica gel with elution by CH_2Cl_2 to yield compound **5** (90 %).

A solution of **5** (1 mmol, 342 mg) in MeOH (24 mL) was treated with the appropriate aldehyde (1.1 mmol) and aqueous KOH (1 mL, 50%), heated at temperature 60^0C for 1.5 h, cooled, diluted with H_2O (up to ~50–60 mL), acidified with HCl (1:4) to pH 3–4, and extracted with CH_2Cl_2 (3 - 10 mL). The extracts were dried over calcined $MgSO_4$. The solvent was removed. The residue was chromatographed over a column of silica gel with elution by CH_2Cl_2.

((4*Z*,10*R*)-12-Acetyl-4-[(2-bromophenyl)methylidene]-8,13-dihydroxy-7,10-dimethyl-5,16-dioxatetracyclo[7.7.0.0$^{2.6}$.0$^{10.15}$]hexadeca-1,6,8,12,14-pentaene-3,11-dione (6e). Yellow amorphous powder.

Yield 58%. M.p. 230 °C dec. Spectrum NMR ^{1}H (400.13 Hz, $CDCl_3$): δ=1.75 (s, 3H, H-15), 2.25 (s, 3H, H-10), 2.65 (s, 3H, H-12), 6.06 (s, 1H, H-4), 7.19 (s, 1H, H-16), 7.19 (t, J = 7.7, 1H, H-20), 7.39 (t, J = 7.7, 1H, H-21), 7.61 (d, J = 7.7, 1H, H-22), 8.23 (d, J = 7.7, 1H, H-19), 11.44 (s, 1H, OH-9), 18.85 (s, 1H, OH-3). NMR ^{13}C (100.61 Hz, $CDCl_3$): δ=7.49 (C-10), 27.90 (C-12), 31.95 (C-15), 58.65 (C-9b), 99.19 (C-4), 100.67 (C-6), 105.11 (C-2), 105.81 (C-8), 108.36 (C-9a), 109.63 (C-16), 126.35 (C-18), 131.92 (CC-17), 127.57, 130.49, 131.84 (C-20, C-21 and C-22), 133.30 (C-19), 148.17 (C-14), 149.89 (C-5a), 159.49 (C-9), 165.63 (C-7), 179.15

(C-4a), 179.49 (C-13), 191.61 (C-3), 197.80 (C-1), 201.82 (C-11). HRMS m/z found: 508.0161 $[M]^+$ $C_{25}H_{17}O_7Br_1$, calcd.: M = 508.0152.

(4*Z*,10*R*)-12-Acetyl-4-[(3-bromophenyl)methylidene]-8,13-dihydroxy-7,10-dimethyl-5,16-dioxatetracyclo[7.7.0.0$^{2.6}$.0$^{10.15}$]hexadeca-1,6,8,12,14-pentaene-3,11-dione (6f). Yellow amorphous powder.

Yield 30%. M.p. 218-219 °C. NMR ^{1}H (400.13 Hz, $CDCl_3$): δ=1.75 (s, 3H, H-15), 2.28 (s, 3H, H-10), 2.65 (s, 3H, H-12), 6.05 (s, 1H, H-4), 6.67 (s, 1H, H-16), 7.29 (dd, 1H, H-19), 7.49 (d, 1H, H-18), 7.72 (d, 1H, H-20), 8.02 (s, 1H, H-22), 11.44 (s, 1H, OH-9), 18.84 (s, 1H, OH-3). NMR ^{13}C (100.61 Hz, $CDCl_3$): δ=7.45 (C-10), 27.84 (C-12), 31.93 (C-15), 58.64 (C-9b), 99.20 (C-4), 100.60 (C-6), 105.10 (C-2), 105.88 (C-8), 108.39 (C-9a), 109.97 (C-16), 122.78 (C-21), 129.55, 130.19, 132.30 and 133.68 (C-18, C-19, C-20 and C-22), 134.17 (C-17), 147.94 (C-14), 149.88 (C-5a), 159.61 (C-9), 165.62 (C-7), 179.21 (C-4a), 179.41 (C-13), 191.59 (C-3), 197.79 (C-1), 201.79 (C-11). HRMS m/z found: 508.0161 $[M]^+$ $C_{25}H_{17}O_7Br_1$, calcd.: M = 508.0152.

(4*Z*,10*R*)-12-Acetyl-4-[(3,5-dibromophenyl)methylidene]-8,13-dihydroxy-7,10-dimethyl-5,16-dioxatetracyclo[7.7.0.0$^{2.6}$.0$^{10.15}$]hexadeca-1,6,8,12,14-pentaene-3,11-dione (6g). Yellow amorphous powder.

Yield 62%. M.p. 176-178 °C. NMR ^{1}H (400.13 Hz, $CDCl_3$): δ=1.79 (s, 3H, H-15), 2.32 (s, 3H, H-10), 2.68 (s, 3H, H-12), 6.08 (s, 1H, H-4), 6.62 (s, 1H, H-16), 7.66 (t, J = 1.7, 1H, H-20), 7.94 (d, J = 1.7, 2H, H-18), 11.53 (s, 1H, OH-9), 18.84 (s, 1H, OH-3). NMR ^{13}C (100.61 Hz, $CDCl_3$): δ =7.41 (C-10), 27.83 (C-12), 31.86 (C-15), 58.60 (C-9b), 99.31 (C-4), 100.40 (C-6), 105.12 (C-2), 105.94 (C-8), 108.31 (C-16), 108.55 (C-9a), 123.11 (2C-19), 132.24 (2C-18), 134.45 (C-20), 135.56 (C-17), 148.48 (C-14), 150.02 (C-5a), 159.75 (C-9), 165.54 (C-7), 179.04 (C-4a), 179.22 (C-13), 191.03 (C-3), 197.78 (C-1), 201.23 (C-11). HRMS m/z found: 585.9250 $[M]^+$ $C_{25}H_{16}O_7Br_2$, calcd.: M = 585.9257.

(4*Z*,10*R*)-12-Acetyl-8,13-dihydroxy-7,10-dimethyl-4-[(3,5-di-tert-butyl-2-hydroxyphenyl)methylidene]-5,16-dioxatetracyclo[7.7.0.0^{2,6}.0^{10,15}]hexadeca-1(9),2(6),7,12,14-pentaene-3,11-dione (6m). Yellow amorphous powder.

Yield 74%. mp 186 °C. $[\alpha]_D^{25.9}$ +197 (c 0.1, $CHCl_3$). NMR ^{1}H (400.13 Hz, $CDCl_3$): δ=1.34 (c, 9H, H-tert-Bu) and 1.46 (c, 9H, H-tert-Bu), 1.74 (s, 3H, H-15), 2.22 (s, 3H, H-10), 2.65 (s, 3H, H-12), 5.99 (s, 1H, H-4), 6.60 (bs, 1H, OH), 7.21 (c, 1H, H-16), 7.40 (c, 1H, H-20), 7.84 (c, 1H, H-22), 11.41 (s, 1H, OH-9), 18.86 (s, 1H, OH-3). NMR ^{13}C (100.61 Hz, $CDCl_3$): δ=7.27 (C-10), 27.93 (C-12), 29.79 and 31.34 (6C-tert-Bu), 31.95 (C-15), 34.29 and 34.88 (2C- tert-Bu), 58.69 (C-9b), 99.14 (C-4), 101.10 (C-6), 105.09 (C-2), 105.64 (C-8), 108.31 (C-9a), 109.03 (C-17), 119.21 (C-16), 126.51 and 126.92 (C-20 and C-22), 136.69 (C-19), 142.61 (C-21), 146.56

(C-14), 149.82 (C-5a), 152.41 (C-18), 159.21 (C-9), 164.96 (C-7), 178.93 (C-4a), 179.58 (C-13), 191.62 (C-3), 197.88 (C-1), 201.85 (C-11). HRMS, found: m/z 558.2246 $[M]^+$ $C_{33}H_{34}O_8$. Calculated: M = 558.2248.

(4*Z*,10*S*)-12-Acetyl-8,13-dihydroxy-7,10-dimethyl-4-[(3,5-di-tert-butyl-2-hydroxyphenyl)methylidene]-5,16-dioxatetracyclo[7.7.0.0^{2,6}.0^{10,15}]hexadeca-1(9),2(6),7,12,14-pentaene-3,11-dione (7m). Yellow amorphous powder. $[\alpha]_D^{25.9}$ -191 (c 0.1, $CHCl_3$).

(4*Z*,10*R*)-12-Acetyl-8,13-dihydroxy-7,10-dimethyl-4-(pyridin-3-ylmethylidene)-5,16-dioxatetracyclo[7.7.0.0^{2,6}.0^{10,15}]hexadeca-1(9),2(6),7,12,14-pentaene-3,11-dione (6o). Yellow amorphous powder.

Yield 66%, mp decomposition >200 ^{0}C, NMR ^{1}H (400.13 Hz, $CDCl_3$): δ=1.75 (s, 3H, H-15), 2.26 (s, 3H, H-10), 2.64 (s, 3H, H-12), 6.04 (s, 1H, H-4), 6.72 (s, 1H, H-16), 7.38 (dd, J = 3.4 and 7.8 Hz, 1H, H-19), 8.18 (d, J = 7.8 Hz, 1H, H-18,), 8.56 (d, J = 3.4 Hz, 1H, H-20), 8.99 (s, 1H, H-21), 11.47 (s, 1H, 9-OH), 18.85 (s, 1H, 3-OH). NMR ^{13}C (100.61 Hz, $CDCl_3$): δ=7.47 (C-10), 27.84 (C-12), 31.88 (C-15), 58.54 (C-9b), 99.24 (C-4), 100.46 (C-6), 105.05 (C-2), 105.87 (C-8), 107.80 (C-16), 108.45 (C-9a), 123.67 (C-18), 128.41 (C-17), 137.38 (C-19), 148.57 (C-14), 149.70 (C-20), 149.88 (C-5a), 151.80 (C-21), 159.69 (C-9), 165.52 (C-7), 178.97 and 179.25 (C-13, C-4a), 191.54 (C-3), 197.71 (C-1), 201.78 (C-11). HRMS, found: m/z 431.1006 [M]+$C_{24}H_{17}NO_7$. Calculated: M = 431.1000.

(4*Z*,10*R*)-12-Acetyl-8,13-dihydroxy-7,10-dimethyl-4-[(1H-pyrrol-2-yl)methylidene]-5,16-dioxatetracyclo[7.7.0.0^{2,6}.0^{10,15}]hexadeca-1(9),2(6),7,12,14-pentaene-3,11-dione (6q). Yellow amorphous powder.

Yield 45%. mp 144-145 ^{0}C. NMR ^{1}H (400.13 Hz, $CDCl_3$): δ=1.75 (s, 3H, H-15), 2.21 (s, 3H, H-10), 2.65 (s, 3H, H-12), 6.04 (s, 1H, H-4), 6.36 (m, 1H, H-19), 6.64 (m, 1H, H-18), 6.96 (s, 1H, H-16), 7.08 (m, 1H, H-20), 11.24 (s, 1H, OH-9), 12.91 (1H, NH), 18.84 (s, 1H, OH-3). NMR ^{13}C (100.61 Hz, $CDCl_3$): δ=7.20 (C-10), 27.88 (C-12), 32.03 (C-15), 58.92 (C-9b), 98.96 (C-4), 102.91 (C-6), 105.10 (C-2), 105.24 (C-8), 107.81 (C-9a), 111.98 (C-18), 114.21 (C-19), 119.14 (C-16), 124.04 (C-20), 126.80 (C-17), 145.07 (C-14), 149.58 (C-5a), 158.39 (C-9), 164.43 (C-7), 177.45 (C-4a), 179.85 (C-13), 191.63 (C-3), 197.92 (C-1), 201.74 (C-11). HRMS, found: m/z 419.1002 $[M]^+$ $C_{23}H_{17}NO_7$. Calculated: M = 419.1005.

(4*Z*,10*R*)-12-Acetyl-8,13-dihydroxy-7,10-dimethyl-4-(furan-2-ylmethylidene)-5,16-dioxatetracyclo[7.7.0.0^{2,6}.0^{10,15}]hexadeca-1(9),2(6),7,12,14-pentaene-3,11-dione (6r). Yellow amorphous powder.

Yield 65%. mp 189-190 °C. NMR ^{1}H (400.13 Hz, $CDCl_3$): δ=1.76 (s, 3H, H-15), 2.29 (s, 3H, H-10), 2.65 (s, 3H, H-12), 6.05 (s, 1H, H-4), 6.59 (s, 1H, H-16), 6.83 (m, 1H, H-19), 7.07

(m, 1H, H-18), 7.58 (m, 1H, H-20), 11.38 (s, 1H, OH-9), 18.83 (s, 1H, OH-3). NMR ^{13}C (100.61 Hz, $CDCl_3$): δ=7.41 (C-10), 27.89 (C-12), 31.96 (C-15), 58.72 (C-9b), 99.13 (C-4), 101.30 (C-6), 100.84 (C-19), 105.13 (C-2), 105.80 (C-8), 108.19 (C-9a), 113.01 (C-18), 116.69 (C-16), 145.03 (C-20), 145.70 (C-14), 148.65 (C-17), 149.67 (C-5a), 159.21 (C-9), 165.30 (C-7), 178.78 (C-4a), 179.63 (C-13), 191.64 (C-3), 197.89 (C-1), 201.81 (C-11). HRMS, found: m/z 420.0839 $[M]^+$ $C_{23}H_{16}O_8$. Calculated: M = 420.0840.

(4*Z*,10*R*)-12-Acetyl-8,13-dihydroxy-7,10-dimethyl-4-(5-methylfuran-2-ylmethylidene)-5,16-dioxatetracyclo[7.7.0.0^{2,6}.0^{10,15}]hexadeca-1(9),2(6),7,12,14-pentaene-3,11-dione (6s). Yellow amorphous powder.

Yield 63%. mp decomposition >220 ^{0}C. NMR ^{1}H (400.13 Hz, $CDCl_3$): δ=1.75 (s, 3H, H-15), 2.26 (s, 3H, H-10), 2.38 (s, 3H, H-21), 2.64 (s, 3H, H-12), 6.03 (s, 1H, H-4), 6.20 (d, 1H, H-19), 6.78 (s, 1H, H-16), 6.98 (d, 1H, H-18), 11.34 (s, 1H, OH-9), 18.81 (s, 1H, OH-3). NMR ^{13}C (100.61 Hz, $CDCl_3$): δ=7.05 (C-10), 13.56 (C-21), 27.54 (C-12), 31.63 (C-15), 58.44 (C-9b), 98.71 (C-4), 101.13 (C-19), 104.78 (C-6), 105.36 (C-2), 106.62 (C-8), 107.74 (C-9a), 109.55 (C-18), 118.44 (C-16), 144.58 (C-17), 146.85 (C-14), 149.48 (C-5a), 155.77 (C-20), 158.62 (C-9), 164.80 (C-7), 178.40 (C-4a), 179.39 (C-13), 191.30 (C-3), 197.60 (C-1), 201.46 (C-11). HRMS, found: m/z 434.0990 $[M]^+$ $C_{24}H_{18}O_8$. Calculated: M = 434.0996.

(4*Z*,10*R*)-12-Acetyl-8,13-dihydroxy-7,10-dimethyl-4-(furan-3-ylmethylidene)-5,16-dioxatetracyclo[7.7.0.0^{2,6}.0^{10,15}]hexadeca-1(9),2(6),7,12,14-pentaene-3,11-dione (6t). Yellow amorphous powder.

Yield 49%. mp decomposition >210 ^{0}C ^{0}C. NMR ^{1}H (400.13 Hz, $CDCl_3$): δ=1.75 (s, 3H, H-15), 2.26 (s, 3H, H-10), 2.64 (s, 3H, H-12), 6.04 (s, 1H, H-4), 6.76 (s, 1H, H-16), 6.87 (s, 1H, H-20), 7.49 (s, 1H, H-19), 7.90 (s, 1H, H-18), 11.38 (s, 1H, OH-9), 18.84 (s, 1H, OH-3). NMR ^{13}C (100.61 Hz, $CDCl_3$): δ=7.28 (C-10), 27.74 (C-12), 31.80 (C-15), 58.55 (C-9b), 98.94 (C-4), 101.16 (C-6), 103.27 (C-20), 104.94 (C-2), 105.42 (C-8), 107.93 (C-9a), 110.59 (C-16), 118.54 (C-17), 143.79 and 145.64 (C-18 and C-19), 147.36 (C-14), 149.52 (C-5a), 159.03 (C-9), 165.16 (C-7), 178.69 (C-4a), 179.45 (C-13), 191.46 (C-3), 197.70 (C-1), 201.64 (C-11). HRMS, found: m/z 420.0838 $[M]^+$ $C_{23}H_{16}O_6$. Calculated: M = 420.0840.

(4*Z*,10*R*)-12-Acetyl-8,13-dihydroxy-7,10-dimethyl-4-(thiofen-2-ylmethylidene)-5,16-dioxatetracyclo[7.7.0.0^{2,6}.0^{10,15}]hexadeca-1(9),2(6),7,12,14-pentaene-3,11-dione (6u). Yellow amorphous powder.

Yield 75%. mp decomposition >220 ^{0}C. NMR ^{1}H (400.13 Hz, $CDCl_3$): δ=1.75 (s, 3H, H-15), 2.31 (s, 3H, H-10), 2.65 (s, 3H, H-12), 6.05 (s, 1H, H-4), 7.10 (s, 1H, H-16), 7.12 (m, 1H, H-19), 7.46 (d, J = 3.6, 1H, H-18), 7.58 (d, J = 5.0, 1H, H-20), 11.38 (s, 1H, OH-9), 18.84 (s, 1H, OH-3). NMR ^{13}C (100.61 Hz, $CDCl_3$): δ=7.53 (C-10), 27.92 (C-12), 31.98 (C-15), 58.74 (C-

9b), 99.12 (C-4), 101.51 (C-6), 105.13 (C-2), 105.90 (C-8), 106.25 (C-16), 108.21 (C-9a), 127.85 (C-19), 131.51 (C-18), 132.72 (C-20), 135.50 (C-17), 145.92 (C-14), 149.66 (C-5a), 159.22 (C-9), 165.28 (C-7), 178.70 (C-4a), 179.63 (C-13), 191.64 (C-3), 197.88 (C-1), 201.82 (C-11). HRMS, found: m/z 436.0608 $[M]^+$ $C_{23}H_{16}O_7S$. Calculated: M = 436.0611.

(4*Z*,10*R*)-12-Acetyl-8,13-dihydroxy-7,10-dimethyl-4-[(5-methylthiofen-2-yl)methylidene]-5,16-dioxatetracyclo[7.7.0.0^{2,6}.0^{10,15}]hexadeca-1(9),2(6),7,12,14-pentaene-3,11-dione (6v). Yellow amorphous powder.

Yield 90%. mp 154-155 ^{0}C. NMR ^{1}H (400.13 Hz, $CDCl_3$): δ=1.75 (s, 3H, H-15), 2.30 (s, 3H, H-10), 2.55 (s, 3H, H-21), 2.65 (s, 3H, H-12), 6.04 (s, 1H, H-4), 6.78 (d, J = 4, 1H, H-19), 7.02 (s, 1H, H-16), 7.26 (d, J = 4, 1H, H-18), 11.34 (s, 1H, OH-9), 18.84 (s, 1H, OH-3). NMR ^{13}C (100.61 Hz, $CDCl_3$): δ=7.50 (C-10), 15.71 (C-21), 27.86 (C-12), 31.93 (C-15), 58.70 (C-9b), 98.97 (C-4), 101.61 (C-6), 105.04 (C-2), 105.74 (C-8), 106.90 (C-16), 107.99 (C-9a), 126.44 (C-19), 133.40 (C-18), 133.47 (C-17), 145.16 (C-14), 147.45 (C-20), 149.48 (C-5a), 158.86 (C-9), 165.09 (C-7), 178.55 (C-4a), 179.66 (C-13), 191.56 (C-3), 197.83 (C-1), 201.73 (C-11). HRMS, found: m/z 450.0769 $[M]^+$ $C_{24}H_{18}O_7S$. Calculated: M = 450.0768.

(4*Z*,10*R*)-12-Acetyl-8,13-dihydroxy-7,10-dimethyl-4-[(3-methylthiofen-2-yl)methylidene]-5,16-dioxatetracyclo[7.7.0.0^{2,6}.0^{10,15}]hexadeca-1(9),2(6),7,12,14-pentaene-3,11-dione (6w). Yellow amorphous powder.

Yield 90%. mp decomposition >220 ^{0}C. NMR ^{1}H (400.13 Hz, $CDCl_3$): δ=1.76 (s, 3H, H-15), 2.32 (s, 3H, H-10), 2.42 (s, 3H, H-21), 2.65 (s, 3H, H-12), 6.06 (s, 1H, H-4), 6.94 (d, J = 4, 1H, H-19), 7.16 (s, 1H, H-16), 7.51 (d, J = 4, 1H, H-20), 11.34 (s, 1H, OH-9), 18.82 (s, 1H, OH-3). NMR ^{13}C (100.61 Hz, $CDCl_3$): δ=7.56 (C-10), 14.46 (C-21), 27.92 (C-12), 31.99 (C-15), 58.76 (C-9b), 99.07 (C-4), 101.69 (C-6), 105.00 (C-16), 105.12 (C-2), 105.91 (C-8), 108.11 (C-9a), 130.12 (C-17), 130.31 (C-19), 130.69 (C-20), 142.75 (C-18), 145.45 (C-14), 149.59 (C-5a), 159.02 (C-9), 165.17 (C-7), 178.68 (C-4a), 179.73 (C-13), 191.64 (C-3), 197.91 (C-1), 201.81 (C-11). HRMS, found: m/z 450.0764 $[M]^+$ $C_{24}H_{18}O_7S$. Calculated: M = 450.0768.

(4*Z*,10*R*)-12-Acetyl-8,13-dihydroxy-7,10-dimethyl-4-(5-bromothiofen-2-ylmethylidene)-5,16-dioxatetracyclo[7.7.0.0^{2,6}.0^{10,15}]hexadeca-1(9),2(6),7,12,14-pentaene-3,11-dione (6x). Yellow amorphous powder.

Yield 94%. mp 162-163 ^{0}C. $[\alpha]_D^{26}$ +259 (c 0.1, $CHCl_3$). NMR ^{1}H (400.13 Hz, DMSO-d_6): δ=1.74 (s, 3H, H-15), 2.21 (s, 3H, H-10), 2.58 (s, 3H, H-12), 6.31 (s, 1H, H-4), 7.21 (s, 1H, H-19), 7.64 (s, 1H, H-16), 7.99 (s, 1H, H-18), 11.82 (s, 1H, OH-9). NMR ^{13}C (100.61 Hz, DMSO-d_6): δ=7.38 (C-10), 27.99 (C-12), 31.35 (C-15), 58.06 (C-9b), 99.16 (C-4), 100.56 (C-6), 104.23 (C-16), 104.41 (C-8), 105.63 (C-2), 109.40 (C-9a), 110.06 (C-20), 129.71 (C-19), 134.65 (C-18), 136.56 (C-17), 146.00 (C-14), 149.55 (C-5a), 158.88 (C-9), 164.34 (C-7), 177.26 (C-4a), 178.95

(C-13), 190.99 (C-3), 197.21 (C-1), 200.98 (C-11). HRMS, found: m/z 513.9714 $[M]^+$ $C_{23}H_{15}O_7BrS$. Calculated: M = 513.9716.

(4*Z*,10*S*)-12-Acetyl-8,13-dihydroxy-7,10-dimethyl-4-(5-bromothiofen-2-ylmethylidene)-5,16-dioxatetracyclo[7.7.0.0^{2,6}.0^{10,15}]hexadeca-1(9),2(6),7,12,14-pentaene-3,11-dione (7x). Yellow amorphous powder. $[\alpha]_D^{26}$ -259 (c 0.1, $CHCl_3$).

(4*Z*,10*R*)-12-Acetyl-8,13-dihydroxy-7,10-dimethyl-4-[(4-bromothiofen-2-yl)methylidene]-5,16-dioxatetracyclo[7.7.0.0^{2,6}.0^{10,15}]hexadeca-1(9),2(6),7,12,14-pentaene-3,11-dione (6y). Yellow amorphous powder.

Yield 68%. mp decomposition >220 ^{0}C. NMR ^{1}H (400.13 Hz, $CDCl_3$): δ=1.76 (s, 3H, H-15), 2.29 (s, 3H, H-10), 2.65 (s, 3H, H-12), 6.05 (s, 1H, H-4), 6.97 (s, 1H, H-16), 7.34 (s, 1H, H-20), 7.44 (s, 1H, H-18), 11.45 (s, 1H, OH-9), 18.86 (s, 1H, OH-3). NMR ^{13}C (100.61 Hz, $CDCl_3$): δ=7.43 (C-10), 27.74 (C-12), 31.97 (C-15), 58.61 (C-9b), 99.16 (C-4), 101.11 (C-6), 104.23 (C-16), 105.07 (C-2), 105.95 (C-8), 108.39 (C-9a), 111.02 (C-19), 127.87 (C-18), 133.82 (C-20), 136.55 (C-17), 146.59 (C-14), 149.75 (C-5a), 159.49 (C-9), 165.21 (C-7), 178.36 (C-4a), 179.38 (C-13), 191.55 (C-3), 197.77 (C-1), 201.72 (C-11). HRMS, found: m/z 513.9713 $[M]^+$ $C_{23}H_{15}O_7BrS$. Calculated: M = 513.9716.

(4*Z*,10*R*)-12-Acetyl-8,13-dihydroxy-7,10-dimethyl-4-(thiofen-3-ylmethylidene)-5,16-dioxatetracyclo[7.7.0.0^{2,6}.0^{10,15}]hexadeca-1(9),2(6),7,12,14-pentaene-3,11-dione (6z). Yellow amorphous powder.

Yield 74%. mp 158-159 ^{0}C. NMR ^{1}H (400.13 Hz, $CDCl_3$): δ=1.75 (s, 3H, H-15), 2.28 (s, 3H, H-10), 2.64 (s, 3H, H-12), 6.04 (s, 1H, H-4), 6.87 (s, 1H, H-16), 7.38 (s, 1H, H-20), 7.56 (s, 1H, H-19), 7.83 (s, 1H, H-18), 11.38 (s, 1H, OH-9), 18.84 (s, 1H, OH-3). NMR ^{13}C (100.61 Hz, $CDCl_3$): δ=7.57 (C-10), 27.96 (C-12), 32.03 (C-15), 58.78 (C-9b), 99.17 (C-4), 101.31 (C-6), 105.16 (C-2), 105.70 (C-8), 106.36 (C-16), 108.19 (C-9a), 126.36, 129.01 and 130.08 (C-18, C-19 and C-20), 133.65 (C-17), 146.74 (C-14), 149.74 (C-5a), 159.27 (C-9), 165.52 (C-7), 179.46 (C-4a), 179.66 (C-13), 191.68 (C-3), 197.92 (C-1), 201.86 (C-11). HRMS, found: m/z 436.0607 $[M]^+$ $C_{23}H_{16}O_7S$. Calculated: M = 436.0611.

(4*Z*,10*R*)-12-Acetyl-8,13-dihydroxy-7,10-dimethyl-4-(cyclohexylmethylidene)-5,16-dioxatetracyclo[7.7.0.0^{2,6}.0^{10,15}]hexadeca-1(9),2(6),7,12,14-pentaene-3,11-dione (6zz). Yellow amorphous powder.

Yield 46%. mp 110 °C. NMR ^{1}H (400.13 Hz, $CDCl_3$): δ=1.23-1.39 (m, 3H, H-19 and H-20 and H-21), 1.73 (s, 3H, H-15), 1.78 (m, 2H, H-18 and H-22), 2.20 (s, 3H, H-10), 2.64 (s, 3H, H-12), 2.69 (m, 1H, H-17), 5.95 (d, J = 9.5, 1H, H-16), 6.04 (s, 1H, H-4), 11.30 (s, 1H, OH-9), 18.83 (s, 1H, OH-3). NMR ^{13}C (100.61 Hz, $CDCl_3$): δ=7.28 (C-10), 25.32 (C-19 and C-21), 25.33 (C-20), 27.87 (C-12), 31.94 (C-15), 31.97 (C-18 and C-22), 35.19 (C-17), 58.74 (C-9b),

99.01 (C-4), 101.56 (C-6), 105.08 (C-2), 105.49 (C-8), 107.61 (C-9a), 121.27 (C-16), 147.99 (C-14), 149.70 (C-5a), 159.17 (C-9), 165.85 (C-7), 179.25 (C-4a), 179.76 (C-13), 191.62 (C-3), 197.91 (C-1), 201.75 (C-11). HRMS, found: m/z 436.1512 $[M]^+$ $C_{25}H_{24}O_7$. Calculated: M = 436.1517.

4.1.2 Synthesis of compound 6l

A solution of 3,4-dihydro-2*H*-pyran (0.67 ml, 7.4 mmol) in dichloromethane (5 mL) was added dropwise into a well-stirred suspension of 4-hydroxybenzaldehyde (300 mg, 2.46 mmol) and pyridinium p-toluene sulfonate (8 mg) in dichloromethane (5 mL). The mixture was stirred at room temperature for 1.5 h, then extracted with brine and dried over $MgSO_4$. The solvent was removed under reduced pressure and the crude compound was purified by column chromatography on silica gel using an elution of 20% EtOAc/hexane to give **6l** as a yellow oil (the yield of compound **8l** 100%).

A solution of **5** (1 mmol, 342 mg) in MeOH (24 mL) was treated with the aldehyde **8l** (1.1 mmol) and aqueous KOH (1 mL, 50%), heated for 1.5 h, diluted with H_2O (up to ~50–60 mL), acidified with HCl (1:4) to pH 3–4, and extracted with CH_2Cl_2 (3 - 10 mL). The extracts were dried over calcined $MgSO_4$. The solvent was removed and the crude compound was dissolved in 10 ml MeOH/CH_2Cl_2. Then the clay K-10 (100 mg) was added and the mixture was stirred at temperature 50 ^{0}C for 2 h. The powder was filtered and the filtrate was evaporated under reduced pressure. The residue was chromatographed over a column of silica gel with elution by 3% MeOH/CH_2Cl_2. The yield of compound **6l** was 78%.

(4*Z*,10*R*)-12-Acetyl-4-[(4-hydroxyphenyl)methylidene]-8,13-dihydroxy-7,10-dimethyl-5,16-dioxatetracyclo[7.7.0.0$^{2.6}$.0$^{10.15}$]hexadeca-1,6,8,12,14-pentaene-3,11-dione (6l). Yellow amorphous powder.

Yield 62%. M.p. 176-178 °C. NMR ^{1}H (400.13 Hz, DMSO-d_6): δ=1.71 (s, 3H, H-15), 2.17 (s, 3H, H-10), 2.61 (s, 3H, H-12), 6.31 (s, 1H, H-4), 6.67 (s, 1H, H-16), 6.84 (d, J = 8, 2H, H-19), 7.72 (d, J = 8, 2H, H-18), 10.19 (s, 1H, OH-20), 11.41 (s, 1H, OH-9), 18.73 (bs, 1H, OH-3). NMR ^{13}C (100.61 Hz, DMSO-d_6): δ=7.49 (C-10), 27.78 (C-12), 31.51 (C-15), 58.53 (C-9b), 98.71 (C-4), 100.62 (C-6), 104.40 (C-2), 105.34 (C-8), 108.83 (C-9a), 112.19 (C-16), 116.13 (2C-19), 122.86 (C-17), 133.45 (2C-18), 145.33 (C-14), 149.282 (C-5a), 158.02 (C-20), 159.54 (C-9), 164.55 (C-7), 177.94 (C-4a), 179.72 (C-13), 191.48 (C-3), 197.88 (C-1), 201.42 (C-11). HRMS m/z found: 446.0990 $[M]^+$ $C_{25}H_{18}O_8$, calcd.: M = 446.1002.

4.2 Biology

4.2.1 Tdp1 assay

The recombinant Tdp1 was purified to homogeneity by chromatography on Ni-chelating resin and phosphocellulose P11 as described[41] using plasmid pET 16B-Tdp1 kindly provided by Dr. K.W. Caldecott (University of Sussex, United Kingdom).

Real-Time Detection of Tdp1 Activity. The Tdp1 activity measurements were carried out as described.[12] The Tdp1-biosensor with a final concentration of 50 nM was briefly incubated in a volume of 200 μL containing Tdp1 buffer (50 mM Tris-HCl pH8.0, 50 mM NaCl, 7 mM β-mercaptoethanol) supplemented with purified 1.3 nM Tdp1 and various concentrations of intibitor. Fluorescence measurements (Ex_{485}/Em_{520} nm) were carried out during the linear phase of reaction (from 0 to 8 min) every 55 sec. The reactions were incubated at a constant temperature of 26 °C in a POLARstar OPTIMA fluorimeter, BMG LABTECH, GmbH. The influence of compounds was evaluated by comparing the fluorescence increase rate in the presence of compounds to that of DMSO control wells. The data were imported into the MARS Data Analysis 2.0 program (BMG LABTECH), and IC_{50} values (concentration of a compound required to reduce the enzyme activity by 50%) were calculated. Tdp1-biosensor 5'-(5,6 FAM-aac gtc agg gtc ttc c-BHQ1)-3' was synthesized in the Laboratory of Biomedical Chemistry, Institute of Chemical Biology and Fundamental Medicine, Novosibirsk, Russia.

Gel-Based Enzyme Assay. Oligonucleotide 5'-([^{32}P]-aac gtc agg gtc ttc c-X)-3', with 5'-radioactive label (X=tyrosine residue or fluorescence quencher BHQ1) was used. The reaction mixture contained 50 nM DNA substrate, 5 nM Tdp1, 50 mM Tris-HCl, 50 mM NaCl, 7 mM β-mercaptoethanol, and the inhibitor **6g** in a concentration 0-30 μM. The reaction was conducted at 25°C for 20 min in the case of 3'-BHQ1 substrate and for 5 min in the case of 3'-tyrosine substrate. The reaction products were separated by electrophoresis in a 20% denaturing polyacrylamide gel with 7M urea. A Typhoon FLA 9500 phosphorimager (GE Healthcare) was used for gel scanning and imaging, and the data were analyzed with QuantityOne 4.6.7 software. IC_{50} values were determined using OriginPro 8.6.0 software.

Synthesis of oligodeoxynucleotide with 3'-attached phosphotyrosine residue. A standard CPG 1000 support for DNA synthesis containing a DMTr-dT residue attached via its 3'-OH group by succinate ester was detritylated, and the 5'-OH group was esterified to the carboxyl group of Nα-Fmoc tyrosine *t*-butyl ether by diisopropyl carbodiimide (DCI) in the presence of 4-dimethylaminopyridine (DMAP). The phenolic OH group was liberated by acid-catalyzed *t*-butyl ether removal in the presence of a fluorinated alcohol as described previously[42,43] while the

Fmoc amino protecting group was retained until the end of solid-phase synthesis. Oligonucleotide synthesis was carried out from the free phenol group of the attached tyrosine by standard β-cyanoethyl phosphoramidite chemistry. The oligonucleotide with a 3'-phosphotyrosine residue was cleaved from support by alkaline hydrolysis, deprotected by usual ammonia treatment and isolated by standard reverse-phased (RP) HPLC using 5'-DMTr group as a purification handle. The RP-HPLC trace of the crude reaction mixture for oligonucleotide purification is shown in Fig. S1 in Supplementary. The identity of the isolated oligonucleotide has been confirmed by mass spectrometry (Fig. S2 in Supplementary).

4.2.2 Cytotoxicity

Tumor cells from human alveolar basal epithelial cells A-549 and embryonic kidney cells HEK-293 (~2000 cells per well) were incubated for 24 h at 37 °C in IMDM medium containing 10% (v/v) fetal bovine serum, 50 U/ml penicillin, 50 mg/ml streptomycin in a humidified atmosphere (5% CO_2), and then they were treated with the tpc and/or UA derivatives in different concentrations. After 72 h of incubation, the relative number of alive cells was determined using 3-[4,5-dimethylthiazol-2-yl]-2,5-diphenyl tetrazolium bromide (standard colorimetric MTT test),[44] and the drug concentration that causes 50% cell death (CC_{50}) was determined. CC_{50} values were determined using OriginPro 8.6.0 software. All values were expressed as mean ± standard deviation (SD) from triplicate experiments performed in a parallel manner. The CC_{50} was determined as the compound concentration required to decrease the A_{570} to 50% of the control (no compound, DMSO), and was determined by interpolation from dose-response curve.

4.3 Molecular Modeling

The molecules were docked to the crystal structure of Tdp1 (PDB ID: 1MU7, resolution 2.0 Å),[45] which was obtained from the Protein Data Bank (PDB).[46] The Scigress Ultra version v2.6[47] program was used to prepare the crystal structure for docking: hydrogen atoms were added, the co-crystalized tungsten(VI) ion and crystallographic water molecules were removed. The Scigress software suite was also used to build the inhibitors, and the MM2[48] force field was used to optimize the structures. The centre of the substrate binding pocket was defined as the position of the hydrogen atom of His263, as its nitrogen formed a coordination bond with the tungsten ion (x = 8.312, y = 12.660, z = 35.452) with 10 Å radius. The centre of the allosteric binding site was defined as the H_α on Ala258 (x = -2.971, y = 24.833, z = 39.768) with 10 Å radius. The molecules were docked at 100% efficiency with fifty docking runs per molecule. The

basic amino acids, lysine and arginine, were defined as protonated, while aspartic and glutamic acids were assumed to be deprotonated. The GoldScore (GS),[33] ChemScore (CS),[34,35] ChemPLP[36] and ASP[37] scoring functions were implemented to validate the predicted binding modes and relative energies of the ligands using the GOLD v5.4 software suite.

The QikProp 3.2[49] software package was used to calculate the molecular descriptors of the compounds. The reliability of QikProp is established for the molecular descriptors. [50]

Acknowledgments

This work was supported by Russian Science Foundation (grant 16-13-10074), excluding the synthesis of the tyrosine-containing solid support and oligonucleotide, which was funded by Russian Science Foundation (grant 15-15-00121 to D. Stetsenko), and grant of Russian Foundation for Basic Research 16-03-00374 to O. Luzina for synthesis of compound **6zz**.

Supplementary data

Supplementary data (RP-HPLC elution profile, mass spectrum of oligodeoxynucleotide with 3'-attached phosphotyrosine residue, and NMR ^{1}H and ^{13}C spectra of compounds **6a–zz**) associated with this article can be found in the online version.

References and notes

[1] Y. Pommier, E. Leo, H. Zhang, C. Marchand. DNA topoisomerases and their poisoning by anticancer and antibacterial drugs. *Chem Biol*. 2010; **17**:421-433.

[2] E. Q. Comeaux, R. C. van Waardenburg. Tyrosyl-DNA phosphodiesterase I resolves both naturally and chemically induced DNA adducts and its potential as a therapeutic target. *Drug Metab Rev*. 2014; **46**:494-507.

[3] S. S. Laev, N. F. Salakhutdinov, O. I. Lavrik. Tyrosyl-DNA phosphodiesterase inhibitors: Progress and potential. *Bioorganic & Medicinal Chemistry*. 2016; **24**: 5017-5027.

[4] T. S. Dexheimer, S. Antony, C. Marchand, Y. Pommier. Tyrosyl-DNA phosphodiesterase as a target for anticancer therapy. *Anticancer Agents Med Chem;* 2008; **8**:381-389.

[5] F. Cortes Ledesma, S. F. El Khamisy, M. C. Zuma, K. Osborn, K. W. Caldecott. A novel human 5'-tyrosyl DNA phosphodiesterase that repairs topoisomerase-mediated DNA damage. *Nature.* 2009; **461**:674-678.

[6] S. Antony, C. Marchand, A. G. Stephen, L. Thibaut, K. K. Agama, R. J. Fisher, Y. Pommier. Novel high-throughput electrochemiluminescent assay for identification of human tyrosyl-DNA phosphodiesterase (Tdp1) inhibitors and characterization of furamidine (NSC 305831) as an inhibitor of Tdp1. *Nucleic Acids Res.* 2007; **35**:4474-4484.

[7] M. Conda-Sheridan, P. V. Narasimha Reddy, A. Morrell, B. T. Cobb, C. Marchand, K. Agama, A. Chergui, A. Renaud, A. G. Stephen, L. K. Bindu, Y. Pommier, M. Cushman. Synthesis and Biological Evaluation of Indenoisoquinolines That Inhibit Both Tyrosyl-DNA Phosphodiesterase I (Tdp1) and Topoisomerase I (Top1). *J Med Chem.;* 2013; **56**:182-200.

[8] V. R. Sirivolu, S. K. Vernekar, C. Marchand, A. Naumova, A. Chergui, A. Renaud, A. G. Stephen, F. Chen, Y. Y. Sham, Y. Pommier, Z. Wang. 5-Arylidenethioxothiazolidinones as Inhibitors of Tyrosyl–DNA Phosphodiesterase I. *J Med Chem.* 2012; **55**:8671-8684.

[9] P. Wang, M. S. A. Elsayed, C. B. Plescia, A. Ravji, C. E. Redon, E. Kiselev, C. Marchand, O. Zeleznik, K. Agama, Y. Pommier, M. Cushman. Synthesis and Biological Evaluation of the First Triple Inhibitors of Human Topoisomerase 1, Tyrosyl−DNA Phosphodiesterase 1 (Tdp1), and Tyrosyl−DNA Phosphodiesterase 2 (Tdp2). *J. Med. Chem*. 2017; **60**: 3275-3288.

[10] A. L. Zakharenko, T. M. Khomenko, S. V. Zhukova, O. A. Koval, O. D. Zakharova, R. O. Anarbaev, N. A. Lebedeva, D. V. Korchagina, N. I. Komarova, V. G. Vasiliev, J. Reynisson, K. P. Volcho, N. F. Salakhutdinov, O. I. Lavrik,. Synthesis and biological evaluation of novel tyrosyl-DNA phosphodiesterase 1 inhibitors with a benzopentathiepine moiety. *Bioorg. Med. Chem.* 2015; **23**:2044-2052.

[11] T. X. Nguyen, M. Abdelmalak, C. Marchand, K. Agama, Y. Pommier, M. J. Cushman. Synthesis and Biological Evaluation of Nitrated 7-, 8-, 9-, and 10-Hydroxyindenoisoquinolines as Potential Dual Topoisomerase I (Top1) − Tyrosyl-DNA Phosphodiesterase I (TDP1) Inhibitors. *J Med Chem;* 2015; **58** (7):3188-3203.

[12] H. J. Arabshahi, M. van Rensburg, L. I. Pilkington, C. Y. Jeon, M. Song, L.-M. Gridel, E. Leung, D. Barker, M. Vuica-Ross, K. P. Volcho, A. L. Zakharenko, O. I. Lavrik, J. Reynisson. A synthesis, in silico, in vitro and in vivo study of thieno[2,3-b]pyridine anticancer analogues. *Med Chem Commun.* 2015; **6**:1987-1997.

[13] I. E. Weidlich, T. Dexheimer, C. Marchand, S. Antony, Y. Pommier, M. C. Nicklaus. Inhibitors of human tyrosyl-DNA phospodiesterase (hTdp1) developed by virtual screening using ligand-based pharmacophores. *Bioorg Med Chem*. 2010; **18** (1):182-189.

[14] D. J. Newman, G. M. Cragg. Natural Products as Sources of New Drugs from 1981 to 2014. *J. Nat. Prod*. 2016; **79**:629−661.

[15] N. F. Salakhutdinov, K. P. Volcho, O. I. Yarovaya. Monoterpenes as a renewable source of biologically active compounds. *Pure & Applied Chem*., 2017; **89**: 1105-1117.

[16] T.S. Dexheimer, L. K. Gediya, A. G. Stephen, I. Weidlich, S. Antony, C. Marchand, H. Interthal, M. Nicklaus, R. J. Fisher, V. C. Njar, Y. Pommier. 4-Pregnen-21-ol-3,20-dione-21-

(4-bromobenzenesulfonate) (NSC 88915) and related novel steroid derivatives as tyrosyl-DNA phosphodiesterase (Tdp1) inhibitors. *J Med Chem*. 2009; **52**(22):7122-7131.

[17] L.-W. Tian, Y. Feng, T. D. Tran, Y. Shimizu, T. Pfeifer, H. T. Vu, R. J. Quinn. Achyrodimer F, a tyrosyl-DNA phosphodiesterase I inhibitor from an Australian fungus of the family Cortinariaceae. *Bioorg. Med. Chem. Lett*. 2017; **27**:4007-4010.

[18] T. Khomenko, A. Zakharenko, T. Odarchenko, H. J. Arabshahi, V, Sannikova, O. Zakharova, D. Korchagina, J. Reynisson, K. Volcho, N. Salakhutdinov, O. Lavrik. New Inhibitors of Tyrosyl-DNA Phosphodiesterase I (Tdp 1) Combining 7-Hydroxycoumarin and Monoterpenoid Moieties. *Bioorganic & Medicinal Chemistry*. 2016; **24**:5573-5581.

[19] A. L. Zakharenko, K. Yu. Ponomarev, E. V. Suslov, D. V. Korchagina, K. P. Volcho, I. A. Vasil'eva, N. F. Salakhutdinov, O. I. Lavrik. *Rus. J. Bioorg. Chem.* 2015; **41**:657-662.

[20] A. Zakharenko, O. Luzina, O. Kova, D. Nilov, I. Gushchina, N. Dyrkheeva, V. Švedas, N. Salakhutdinov, O. Lavrik. Tyrosyl-DNA Phosphodiesterase 1 Inhibitors: Usnic Acid Enamines Enhance the Cytotoxic Effect of Camptothecin. *J. Nat. Prod.* 2016; **79**:2961-2967.

[21] O. A. Luzina, N. F. Salakhutdinov. Biological Activity of Usnic Acid and Its Derivatives: Part 1. Activity against Unicellular Organisms. *Russ J Bioorg Chem*. 2016; **42**:115-132.

[22] O. A. Luzina, N. F. Salakhutdinov. Biological Activity of Usnic Acid and its Derivatives: Part 2. Effects on Higher Organisms. Molecular and Physicochemical Aspects. *Russ J Bioorg Chem*. 2016; **42**:249-268.

[23] M. Bruno, B. Trucchi, D. Monti, S. Romeo, M. Kaiser, L. Verotta. Synthesis of a potent antimalarial agent through natural products conjugation. *ChemMedChem.* 2013; **8**:221-225.

[24] A. A. Shtro, V. V. Zarubaev, O. A. Luzina, D. N. Sokolov, O. I. Kiselev, N. F. Salakhutdinov. Novel derivatives of usnic acid effectively inhibiting reproduction of influenza A virus. *Bioorg. Med. Chem.* 2014; **22**:6826-6836.

[25] O. B. Bekker, D. N. Sokolov, O. A. Luzina, N. I. Komarova, Y. V. Gatilov, S. N. Andreevskaya, T. G. Smirnova, D. A. Maslov, L. N. Chernousova, N. F. Salakhutdinov, V. N. Danilenko. Synthesis and activity of (+)-usnic acid and (−)-usnic acid derivatives containing 1,3-thiazole cycle against Mycobacterium tuberculosis. *Medicinal Chemistry Research* 2015; **24**(7):2926-2938.

[26] A. N. Abo-Khatwa, A. A. Al-Robai, D. A. Al-Jawhari. Lichen Acids as Uncouplers of Oxidative Phosphorylation of Mouse-Liver Mitochondria. *Natural Toxins*. 1996; **4**:96-102.

[27] O. A. Luzina, D. N. Sokolov, A. V. Shernyukov, N. F. Salakhutdinov. Synthesis of aurones based on usninic acid. *Chem Nat Compd.* 2012; **48**:385-391.

[28] H. Berman; K. Henrick; H. Nakamura. Announcing the worldwide Protein Data Bank. *Nat. Struct. Biol.* 2003; **10**: 980.

[29] J. Dancey, E. A. Eisenhauer. Current perspectives on camptothecins in cancer treatment. *Br. J. Cancer*. 1996; **74**: 327-338.

[30] D. Lorusso, A. Pietragalla, S. Mainenti, V. Masciullo, G. Di Vagno, G. Scambia. Review role of topotecan in gynaecological cancers: current indications and perspectives. *Crit. Rev. Oncol. Hematol*. 2010;**74**:163-174.

[31] M. O'Brien, J. Eckardt, R. Ramlau. Recent advances with topotecan in the treatment of lung cancer. *Oncologist*. 2007; **12**:1194-1204.

[32] D. R. Davies, H. Interthal, J. J. Champoux, W. G. J. Hol. Crystal Structure of a Human Tyrosyl-DNA Phosphodiesterase (Tdp1)-Tungstate Complex. *J. Mol. Biol*. 2003; **324**: 917–932.

[33] G. Jones, P. Willet, R. C. Glen, A. R. Leach, R. Taylor. Development and Validation of a Genetic Algorithm for Flexible Docking. *J.Mol.Biol.* 1997; **267**:727-748.

[34] M. D. Eldridge, C. Murray, T. R. Auton, G. V. Paolini, P. M Mee. Empirical scoring functions: I. The development of a fast empirical scoring function to estimate the binding affinity of ligands in receptor complexes. *J Comp Aid Mol Design.* 1997; **11**:425-445.

[35] M. L. Verdonk, G. Chessari, J. C. Cole, M. Hartshorn, C. W. Murray, J. W. M. Nissink, R. D. Taylor, R. Taylor. Modelling Water in Protein-Ligand Docking Using GOLD. *J Med Chem.* 2005; **48**:6504-6515.

[36] O. Korb, T. Stutzle, T. E. Exner. Empirical Scoring Functions for Advanced Protein−Ligand Docking with PLANTS. *J Chem Inf Model.* 2009; **49**:84-96.

[37] W. T. M. Mooij, M. L. Verdonk. General and targeted statistical potentials for protein–ligand interactions. *Proteins.* 2005; **61**(2):272-287.

[38] T. S. Dexheimer, S.-Y. N. Huang, B. B. Das, Y. Pommier. Tyrosyl-DNA-Phosphodiesterase. In: Pommier Y. *DNA Topoisomerases and Cancer*. Springer New York: New York, NY; 2012:335-354.

[39] F. Zhu, G. Logan, J. Reynisson. Wine Compounds as a Source for HTS Screening Collections. A Feasibility Study. *Mol. Inf.*, 2012; **31**:847-855.

[40] N. F. Salakhutdinov, M. P. Polovinka, M. Y. Panchenko. RU Pat. No. 2,317,076 C1, *Byull. Izobret.* 2008; No 5.

[41] H. Interthal, J. J. Pouliott, J. Champoux. The tyrosyl-DNA phosphodiesterase Tdp1 is a member of the phospholipase D superfamily. *J Proc Natl Acad Sci. USA.* 2001; **98**:12009-12014; N. A. Lebedeva, N. I. Rechkunova, O. I. Lavrik. AP-site cleavage activity of tyrosyl-DNA phosphodiesterase 1. *FEBS Lett.* 2011; **585**:683-686.

[42] D. A. Stetsenko, V. S. Apukhtina, B. P. Chelobanov, P. Palladino. Removal of acid-labile protecting or anchoring groups in the presence of polyfluorinated alcohol: application to solid-phase peptide synthesis. *Russ J Bioorg Chem.* 2016; **42**(2):143-152.

[43] P. Palladino, D. A. Stetsenko. New TFA-free cleavage and final deprotection in Fmoc solid-phase peptide synthesis: dilute HCl in fluoro alcohol. *Org Lett;* 2012; **14**(24):6346-6349.

[44] T. J. Mosmann. Rapid colorimetric assay for cellular growth and survival: application to proliferation and cytotoxicity assays. *Immunol Methods.* 1983; **65**:55-63.

[45] D. R. Davies, H. Interthal, J. J. Champoux, W. G. J. Hol. The Crystal Structure of Human Tyrosyl-DNA Phosphodiesterase, Tdp1. *Structure.* 2002; **10** (2):237-248.

[46] H. M. Berman, J. Westbrook, Z. Feng, G. Gilliland, T. N. Bhat, H. Weissig, I. N. Shindyalov, P. E. Bourne. The Protein Data Bank. *Nucl Acids Res.* 2000; **28**:235-242.

[47] *Scigress v2.6*, Fijitsu Limited: 2008-2016.

[48] N. L. Allinger, Conformational analysis. 130. MM2. A hydrocarbon force field utilizing V1 and V2 torsional terms. *J Am Chem Soc.* 1977; **99**:8127-8134.

[49] QikProp *v3.2*, Schrödinger, New York, 2009.

[50] L. Ioakimidis, L. Thoukydidis, S. Naeem, A. Mirza, J. Reynisson. Benchmarking the Reliability of QikProp. Correlation between Experimental and Predicted Values. *QSAR Comb. Sci.*, 2008; **27**:445-456.

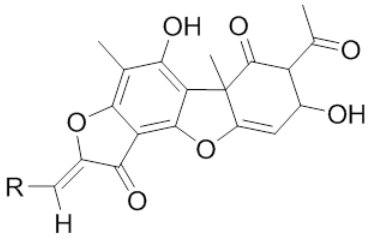

IC_{50} against Tdp1 from 25 nM to 5.5 µM